FORMATION OF ELECTRON BUNCHES FOR HARMONIC CASCADE X-RAY FREE ELECTRON LASERS

M. Cornacchia, S. Di Mitri, G. Penco, Sincrotrone Trieste, Trieste, Italy
A.A. Zholents [#], LBNL, Berkeley, CA 94720, U.S.A.

Abstract

Specific requirements for the electron beam in harmonic cascade free electron lasers, together with means to produce such beams, are presented.

INTRODUCTION

The operation of x-ray free electron lasers (FELs) relies on extremely high quality electron beams. Two FEL projects employing the technique of self-amplified spontaneous emission define the state-of-the-art situation: peak current of few kilo-amperes, emittance of 1 mm-mrad or less, and an energy spread of 1 MeV or less [1,2]. Creation of electron bunches with these parameters is a difficult and elaborate process consisting of the electron bunch production, acceleration and compression. A significant understanding was gained in the underlying physics over the past decade [3-8]. The main phenomena affecting electron bunches include space charge effects, wake-fields and coherent synchrotron radiation (CSR). Nonlinearity of the waveform of the accelerating field in the linac and nonlinear time-of-flight characteristics of bunch compressors also play an important role.

More demanding for the electron beam quality are FELs that are designed to generate temporally coherent x-rays. These FELs, called high-gain harmonic generation FELs or simply harmonic cascade FELs (HC FELs) [9-11], employ a laser to seed the radiation at a lower harmonic of the output FEL radiation. Very often several FEL cascades are used to obtain the radiation at the x-ray wavelength. In these cases the radiation produced in one cascade by one group of electrons proceeds ahead and interacts with other electrons from the same electron bunch in the next cascade. Thus, relatively long electron bunches are needed to accommodate this technique. It is important to have a constant (flat) peak current over the bunch length and a discussion of means to obtain it is one of the objectives of this paper.

HC FELs are often considered for the production of relatively long temporally coherent x-ray pulses with a narrow bandwidth. However, in order to fully realize this potential performance, one must make sure that there is no frequency chirp in the signal (or as little as possible). This chirp can be caused either by energy modulation along the electron bunch [12,13] or by frequency chirp in the seeding laser. In this paper the origins of the energy modulation and means to obtain flat distributions are discussed. The goal is to obtain flat-flat distribution, *i.e.* flat in both peak current and energy. It is also important to avoid or to significantly reduce peak current spikes at the edges of the electron bunch. Those spikes often occur after the final bunch compression.

REVERSE TRACKING

The micro-bunching instability and the resultant energy modulation of electrons with wavelengths in the 10-50 μm region has received a lot of attention in the past (see, [14,15] and references therein). Possible causes of energy modulation on a larger scale , comparable to the bunch length, are discussed in this paragraph, together with means to control them.

The basic premise is that the output bunch configuration is largely pre-determined by the input bunch configuration and, thus, it is possible to find a unique electron density distribution at the beginning of the linac that produces a flat-flat distribution at the end of linac. Finding this distribution can be relatively easy. One just needs to reverse the problem, *i.e.* start at the end of the linac and move backwards towards the beginning of the linac. Eq.(1) shows that for a given electron density λ_z and wake function w, the electron energy at the end of a section of the linac, defined as δ_f (with s_f being the electron coordinate taken with respect to the bunch center), can be determined using the electron energy δ_i and the coordinate s_i at the beginning of the section:

$$\delta_f(s_f) = \delta_i(s_i) + eU\cos(ks_i + \phi) - Q\int_s^\infty w(s-s')\lambda_z(s')ds' \quad (1)$$

where U, ϕ, k define the rf voltage, phase and wave number and e is the electron charge and Q .is the bunch charge For a relativistic beam the electron distribution function λ_z does not change during acceleration, *i.e* $s_f \equiv s_i$, and, therefore, Eq.(1) can be used to define $\delta_i(s_i)$ as a function of $\delta_f(s_f = s_i)$. Thus, beginning with a desirable electron distribution at the end of the linac section, one can find the distribution at the beginning of the linac section that will eventually make it.

A different situation arises in a bunch compressor where the electron coordinate at the end of the bunch compressor $s_f(\delta_f)$ becomes a function of the electron coordinates s_i and energy δ_i at the beginning of the bunch compressor:

$$s_f(\delta_f) = s_i + R_{56}\delta_i + T_{566}\delta_i^2 + f_{CSR}(s_i,\delta_i) \quad ... \quad (2)$$

where R_{56}, T_{566} are first and second order time-of-flight parameters and a function f_{CSR} describes changes related to the CSR effects. In the case of a smooth electron density distribution, the emission of synchrotron radiation is coherent at frequencies $\omega \le c/\ell_b$, where c is the speed

AAZholents@LBL.GOV

of light and ℓ_b is the characteristic length of the scale of the bunch length [16]. Because the electron bunch moves inside the vacuum chamber, most of spectral components of the CSR do not propagate if ℓ_b is long, as it is often the case of HC FEL. Therefore, the loss of electron energy due to CSR is often much smaller than otherwise expected in a free space environment (see Figure 1).

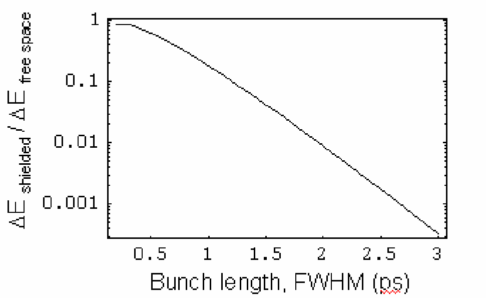

Figure 1: Suppression of CSR due the shielding effect from the vacuum chamber with a gap of 8 mm. This result was obtained by following the recipe proposed in [17].

Thus, if one ignores CSR and assumes that the electron energy is not affected in the magnets of the bunch compressor, i.e. $\delta_f \equiv \delta_i$, then the electron coordinate at the beginning of the bunch compressor can be found using the electron coordinate at the end of the bunch compressor using Eq.(2).

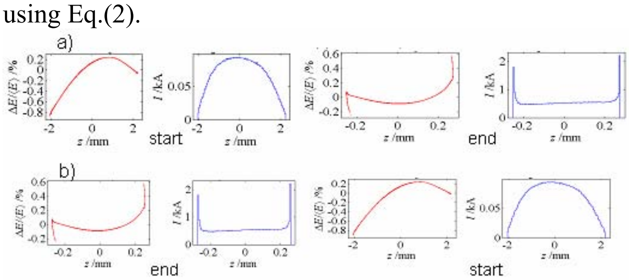

Figure 2: Plot a) shows forward particle tracking and plot b) shows reverse particle tracking.

The above considerations justify a concept of reverse tracking demonstrated in Figure 2. Fig.2a shows the result of conventional forward particle tracking obtained with LiTrack [18] starting with the particle distribution at the beginning of the linac and Fig.2b shows the reverse tracking starting with the distribution obtained at the end of the first tracking (see top right and bottom left sections of the Fig.2). The result of this tracking (bottom right section) agrees well with the initial distribution (top left section).

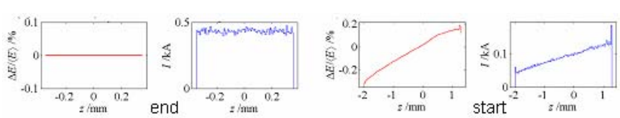

Figure 3: Reverse tracking beginning with flat-flat distribution at the end of the accelerator (end) and moving towards beginning of the accelerator (start).

In the next step, a desirable flat-flat distribution was set-up at the end of the accelerator. Starting with this distribution and tracking it backward, the nearly linear ramped peak current shown in Figure 3 was obtained at the start of the accelerator.

This result can be understood if one uses the wake function for an accelerating section consisting of an array of cells [19]:

$$w(s) = A\frac{Z_0 c}{\pi a^2}\exp\left(-\sqrt{s/s_0}\right) \tag{3}$$

and convolute it with the linear ramped peak current distribution shown with the red line in Fig. 4a to obtain the wake potential

$$W(s) = -\int_s^\infty w(s-s')\lambda_z(s')ds' \tag{4}$$

shown with the red line in Fig. 4b. Here a is the iris radius, Z_0=377Ω and $A \approx 1$ and s_0 are fitting coefficients. As seen in Fig.4b, the wake potential is highly linear and this is why the final distribution is flat in energy.

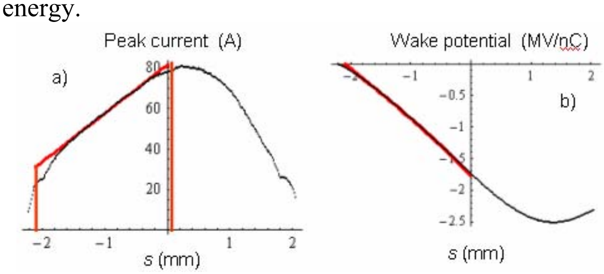

Figure 4: Density distribution with a linear ramped peak current (a) and a correspondent wake potential (b). The red line shows a desirable ideal distribution and its associated wake potential. The black line shows the realistic density distribution obtained in the studies of the photo-injector using the laser pulse with a quadratic ramp in the intensity (a), and the wake potential that corresponds to that distribution (b). The part under the red line contains approximately 40% of the total charge containing under the black line.

Now consider a condition that allows a conversion of a linear ramped peak current at the beginning of the accelerator into the flat distribution at the end of the compression. A compression factor can be defined as $C = I_a / I_b$, where I_a is the peak current after compression and I_b is the peak current before compression. A transformation from a linear ramped peak current $I_b = I_{b0} + I_b' s$ to the flat distribution $I_a = I_{a0}$=Const can be obtained with:

$$C^{-1} = I_{b0}/I_{a0} + s\,I_b'/I_{a0}, \tag{5}$$

i.e. with a compression factor that gradually decreases from the head to the tail of the electron bunch. On the other side $C^{-1} = 1 + hR_{56}$, where $h = d(\Delta E/E)/ds$ is the energy chirp in the electron bunch. Thus, Eq.(5) can be realized if one uses the energy chirp with a quadratic component, i.e. $h = h_0 + h's$, where $h'R_{56} = I_b'/I_{a0}$.

This result can be easily generalized. For example, in some cases a distribution with the maximum peak current at the head of the bunch gradually reducing towards the tail can be beneficial for HC FEL, *i.e.* one may want

$I_a = I_{a0} - I'_a s$. Performing a similar analysis, one can find that this distribution can be obtained with a slight modification to the quadratic energy chirp $h' R_{56} = I'_b / I_{a0} + I'_a I_{b0} / I_{a0}^2$.

BIFURCATION IN PHASE SPACE AND PEAK CURRENT SPIKES

The peak current spikes at the edges of the compressed electron bunches are largely due to the compressor's second order time-of-flight parameter T_{566} and the cubic chirp in the electron energy distribution $\mu = d^3E/ds^3$. Both of them cause the bifurcation in the phase space whose example is shown in Figure 5b. Controlling μ is likely the only way to control the bifurcation for a given R_{56} since T_{566} is often bound to $T_{566} \approx -3/2R_{56}$ if sextupoles are not used in the bunch compressor.

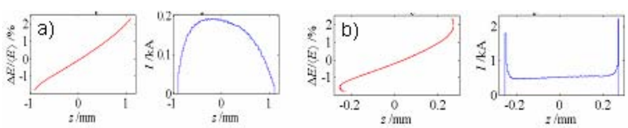

Figure 5. Electron distribution in the longitudinal phase space: a) before bunch compressor, b) after the bunch compressor.

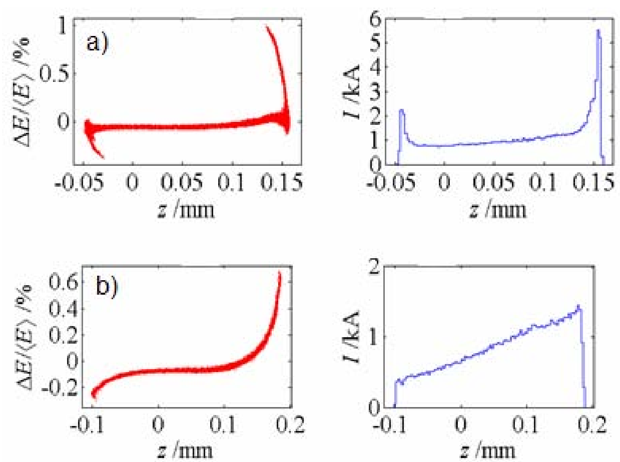

Figure 6: Longitudinal phase space and peak current distributions: a) μ=-0.008 MeV/mm^3, b) μ=-0.088 MeV/mm^3.

Figure 6 shows a typical example that demonstrates how the change in μ from -0.008 MeV/mm^3 to -0.088 MeV/mm^3 in the electron energy distribution created in the injector removes the bifurcation after the bunch compressor. Related to that is a drop of the spikes in the peak current from ~5 kA. in the first case to approximately no spikes condition in the second case. Apart from the cubic energy chirp, the same initial distributions were used in both cases.

It should be pointed out that the distribution in Fig.6a is "flat" in energy and in peak current, while the distribution in Fig.6b is neither "flat" in the energy nor it is "flat" in the peak current. By using cubic energy chirp as a knob one can obtain either flat-flat distributions or distributions without spikes rather routinely, but not both features at the same time. Simply having just one knob is not enough. However, one can effectively employ the peak current distribution in the gun to provide needed μ using the wake fields. In the case of strong wake fields this method was found to be much more effective than correction using high harmonic cavity [20]. This approach already gave good results in the case of the distribution shown with the black line in Fig.4a.

CONCLUSION

In the presence of the wake fields, the electron density distribution plays an important role in formation of the electron bunches at the end of the accelerator. Often, abilities to manipulate the electron density during acceleration and compression are very limited and cannot provide a desirable effect. However, use of the laser in the photocathode gun opens a new opportunity to affect the electron density distribution by controlling its intensity. This paper provides a practical example where the electron density distribution with a linear ramped peak current, obtained through a quadratic ramp in the laser intensity, had many useful implications.

Acknowledgement. We are grateful to P. Emma, G. Stupakov and C. Pellegrini for many useful discussions.

REFERENCES

[1] *LCLS CDR*, SLAC Report No. SLAC-R-593, 2002.
[2] *TESLA TDR*, DESY Report No. DESY-2001-011, 2001.
[3] M. Borland *et al.*, NIM A **483**, 268 (2002).
[4] E.L. Saldin, E.A. Schneidmiller, and M.V. Yurkov, NIM A **490**, 1 (2002).
[5] S. Heifets, G. Stupakov, and S. Krinsky, Phys. Rev. ST Accel. Beams **5**, 064401 (2002).
[7] Z. Huang *et al.*, PRST AB **7**, 074401 (2004).
[8] K. Bane, SLAC-PUB-11829, 2006.
[9] R. Bonifacio, L. De Salvo Souza, E.T. Scharlemann, *NIM A*, **296**, 787(1990).
[10] L.-H. Yu *et al.*, *Science*, **289**, 932 (2000).
[11] G. Penn *et al.,* Proc. of EPAC 2004, Lucerne (2004).
[12] S. G. Biedron, S.V. Milton, and H.P. Freund, NIM A **475** (2001)401.
[13] T.Shaftan *et al.,* Phys. Rev. E, **71**, (2005)046501.
[14] Z. Huang and K.-J. Kim, Phys. Rev. ST Accel. Beams **5**, 074401 (2002).
[15] Z. Huang *et al*., PRST-AB, 074401, 2004.
[16] L.I. Schiff, Rev. Sci. Instr. **17** (1946)6.
[17] R.Li, C.L. Bohn, J.J. Bisongnano, Proc. Particle Accelerator Conference 1997, (1997)1644.
[18] K.L.F. Bane P. Emma, Proc. PAC2005, Knoxville, Tennessee, (2005)4266.
[19] K. Bane, A. Mosnier, A. Novokhatski, K. Yokoya, Proc. ICAP Conf., Monterey, (1998).
[20] K. Flottmann, T. Limberg, Ph. Piot, TESLA-FEL-2001-06.